Dynamics of carrier transport and carrier capture in $In_{1-x}Ga_xAs/InP$ heterostructures

R. Kersting, R. Schwedler, K. Wolter, K. Leo, and H. Kurz
Institut für Halbleitertechnik II, Rheinisch-Westfälische Technische Hochschule Aachen, Sommerfeldstrasse 24, W-5100 Aachen, Germany
(Received 3 February 1992)

We investigate the carrier-transfer dynamics in $In_{1-x}Ga_xAs/InP$ heterostructures using luminescence upconversion spectroscopy with 300-fs time resolution. Carrier transport across the InP barriers to the quantum wells and the final carrier capture into confined states of the quantum wells are separated in a comparative study of samples of different well and barrier thicknesses. The transport of carriers across the barrier material to the quantum wells is found to be almost instantaneous for barrier thicknesses up to 30 nm. We obtain capture-time constants of about 800 fs for electrons and 200 fs for holes. The capture times are virtually independent of well width. We develop a formalism to calculate the carrier transfer time from the barriers to the quantum wells for given well and barrier thicknesses. An upper limit of modulation frequencies set by this transfer process of the order of 300 GHz for devices with thin barriers is derived.

I. INTRODUCTION

$In_{1-x}Ga_xAs/InP$ heterostructures have recently gained great interest as a basis material for optoelectronic devices applications. This material system allows the energetic adjustment of radiative transitions of the $In_{1-x}Ga_xAs$ quantum wells (QW's) to the wavelengths of minimal absorption (1.55 μm) and zero dispersion (1.3 μm) of commercial silica optical fibers. Ultrafast electro-optical and all-optical switching based on nonlinear processes, like gain compression or the intensity dependent refractive index near the band edge, are possible. The maximum modulation frequency of devices is controlled by the picosecond and subpicosecond dynamics of nonequilibrium carriers. Many groups have recently investigated the nonequilibrium carrier thermalization, relaxation and cooling in $In_{1-x}Ga_xAs$ (Refs. 1–5) and InP.[6–9] Another important process limiting the operational speed of heterostructures is the charge transfer from the barrier material into the QW's. In a simple picture, the carrier transfer can be divided in two time-sequential processes, carrier transport and carrier capture: In a first step, free carriers are transported from the InP barriers to the QW's; in a second step, the carriers are captured into the QW's by a scattering process from the unbound three-dimensional to the quasi-two-dimensional states confined in the QW's. A basic limit to the maximum modulation speed of a device is the speed of this transfer process. A detailed knowledge of the dynamics of both transport to the wells and capture into the wells is therefore desirable for the design of ultrafast optoelectronic and photonic devices. Time-resolved optical experiments allow a direct observation of ultrafast carrier dynamics in semiconductors with picosecond and subpicosecond time resolutions. A particular suitable technique is luminescence upconversion with femtosecond time resolution, which provides direct information on the dynamics of carrier relaxation, capture and transport.

In $Al_xGa_{1-x}As/GaAs$ heterostructures the first measurements of the carrier capture performed by Göbel and co-workers[10] demonstrated fast and efficient transfer from the barriers to the wells. Time-resolved luminescence measurements of Feldmann *et al.*[11] and Polland *et al.*[12] performed on graded index separate confinement heterostructures yielded transfer times of less than 20 ps and a dependence of the efficiency on the confinement structure. The measurements and calculations of Blom *et al.*[13] for $Al_xGa_{1-x}As/GaAs$ separate confinement heterostructures gave ambipolar transfer times of 20 ps for electrons and holes. Based on a diffusion model, local capture times of 3 ps were deduced. $In_{1-x}Ga_xAs/InP$ heterostructures were investigated by Westland *et al.*[14] with time-resolved luminescence experiments. A comparison with model calculations based on a capture process combined with a diffusive transport gave capture times of 4 ps.

More direct measurements of the transfer process were performed in $In_{1-x}Ga_xAs/InP$ QW's by Deveaud *et al.*[15] using luminescence upconversion experiments with subpicosecond time resolution. Both QW luminescence and InP barrier luminescence were observed. Total transfer times of 2–3 ps were observed and interpreted by diffusive carrier transport across the barrier material. Quantum capture times were estimated to be 300 fs for holes and 1 ps for electrons. These conclusions are in contrast to our earlier results, which show that the diffusive transport across the InP barriers does not restrict the carrier transfer for structures with barrier widths up to 30 nm.[16]

In addition to the time-resolved studies, a number of steady-state luminescence experiments have been performed. Cathodoluminescence studies were per-

formed by Christen *et al.*[17] and Bimberg *et al.*[18] on $Al_xGa_{1-x}As/GaAs$ multiple quantum wells (MQW's). Very short (100 and 660 fs for electrons and holes, respectively) carrier transfer times were estimated by comparison of the time-integrated luminescence intensities of the $Al_xGa_{1-x}As$ barriers and the GaAs QW's. By a similar comparison of the cw-luminescence intensity ratios of QW's and barriers, Reihlen *et al.*[19] measured a transfer time of 5 ps attributed to a fast depletion of the 200-nm barriers by electron diffusion. A resonant behavior of the carrier capture for certain well widths was observed by Ogasawara *et al.* and Fujiwara *et al.*[20,21] using cw-photoluminescence excitation experiments in the $Al_xGa_{1-x}As/GaAs$ material system. However, all cw measurements suffer from the indirect determination of the dynamics, which can be incorrect because of the quantum efficiencies of the QW and barrier luminescence.

Theoretical calculations of capture processes are based on a scattering process by longitudinal optical-phonon emission.[22–24] Strong oscillations of the capture rate with increasing well width are predicted. The oscillations occur when confined levels move into the QW continuum with decreasing well width. The theoretically evaluated capture times range from 1 to 500 ps for $Al_xGa_{1-x}As/GaAs$ heterostructures. An inclusion of the confined phonon modes within the QW's in the calculations results in further resonances.[24] Recently, Blom, Haverkort, and Wolter[25] have studied theoretically the capture in MQW's within a separate confinement structure. The results indicate that a suitable design of the structure can enhance the carrier transfer process considerably.

The experimental and theoretical results mentioned show that the detailed understanding of the transfer process in semiconductor heterostructures is still incomplete. In this work, we present a detailed analysis of the carrier transfer process in $In_{1-x}Ga_xAs/InP$ heterostructures using femtosecond luminescence upconversion. A large number of samples with different well and barrier widths are compared to obtain a complete picture for the transfer dynamics in this material system. The relaxation of the carriers within the barriers and the wells is studied by analyzing the hot luminescence spectra as a function of time. It turns out that the carrier distributions in wells and barriers have very similar temperatures and cool rather quickly to temperatures close to the lattice temperature. The charge transfer is directly observed by the temporal increase of the QW and the complementary decrease of the barrier luminescence. The capture speed and efficiency is virtually constant over a large range of well widths. No resonances of the transfer time are observed, in contrast to theoretical studies. For barrier widths smaller than about 30 nm, the transport across the barriers does not limit the transfer speed. The experimental results are well reproduced by simple model calculations. The capture times obtained from this analysis are about 800 fs for electrons and 200 fs for holes, respectively.

The paper is organized as follows: In Sec. II the sample structures and characterization are described. The photoluminescence upconversion apparatus is briefly explained. In Sec. III results about the initial carrier relaxation in the InP barriers and the $In_{1-x}Ga_xAs$ QW's are presented. Section IV describes a model calculation of carrier capture and transport. In Sec. V our experimental results are compared with the model and previous results in the literature. Finally, we present a simple formalism to estimate the transfer times for heterostructures with barrier widths up to 30 nm. The paper is concluded with a brief summary in Sec. VI.

II. EXPERIMENT

Two sets of lattice matched $In_{1-x}Ga_xAs/InP$ multiple-quantum-well (MQW) samples grown by low pressure metal-organic vapor-phase epitaxy are compared. The first set contains 10 periods of 30-nm barriers and QW's of various width. The $In_{1-x}Ga_xAs$ well widths range from 0.5 to 6 nm. Using this set, the dependence of the carrier transfer on well width and excitation density is investigated. The transport across the barrier material is studied with a second set of MQW's with a fixed well width of 2.5 nm and barrier widths between 10 and 120 nm. All samples are covered by a 60-nm InP cap layer.

Details of the growth process have already been published elsewhere.[26,27] The alloy composition of the $In_{0.47}Ga_{0.53}As$ as well as the growth of the InP are determined by x-ray diffraction and cw-photoluminescence measurements. Low-temperature exciton luminescence line widths of 2 meV for the $In_{1-x}Ga_xAs$ and 0.63 meV for the InP demonstrate the high quality of the layers.[26] The luminescence spectra of the heterostructures reveal exciton EH_1 transitions split in several discrete peaks. By comparison of the luminescence position for a set of well widths, these lines allow a reproducible identification of the $In_{1-x}Ga_xAs$ layer thickness in steps of monolayers (ML).[28] The fluctuations of the well width are found to be less than 0.5 ML on a scale smaller than the exciton area and approximately 1 ML over the luminescence spot size.[26,27,29,30]

All time-resolved data presented here were obtained by photoluminescence upconversion experiments. Our setup (Fig. 1) differs only in minor details from the schemes described in Refs. 31–33. Two beams of a colliding-pulse mode-locked ring dye laser[34,35] (CPM) with a central wavelength of about 630 nm and a pulse duration of 80 fs are used. The pulse energy and the repetition rate are 300 pJ and 90 MHz, respectively, corresponding to an average power of 25 mW per beam. Using one beam for the excitation, carrier densities between 10^{16} and 10^{19} cm^{-3} can be generated in the samples. The emitted luminescence is focused onto a β-barium borate (BBO) crystal. Sum-frequency light is generated when luminescence and reference pulse have temporal overlap within the nonlinear crystal. The sum-frequency light is dispersed by a monochromator and detected by a single-photon counting system. The temporal evolution of the luminescence signal is mapped by delaying the reference pulse with respect to the pulse exciting the sample.

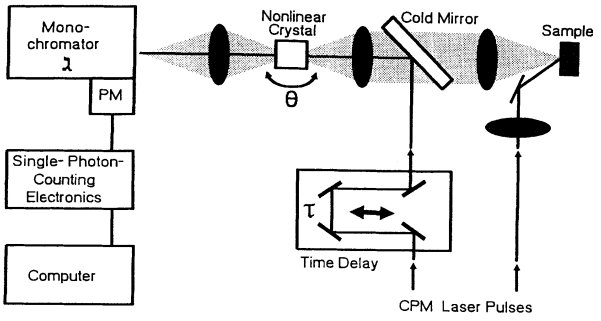

FIG. 1. Luminescence upconversion setup.

The group-velocity dispersion (GVD) of the lens system focusing the luminescence onto the BBO induces time shifts of up to 3 ps for different luminescence energies. Calculations of the lens dispersion as well as measurements at different luminescence energies show that these delays are reproducible. We correct the GVD of the lens system with the computer control of the experimental apparatus with an accuracy better than 100 fs.

Apart from the pulse duration of the CPM pulse the time resolution of the setup is limited by different GVD between the infrared luminescence and the reference pulse within the nonlinear crystal. We chose BBO because detailed calculations show that 2.5 times higher quantum efficiencies can be achieved with BBO than with lithium iodate under comparable conditions of GVD. In our measurements, we use a 1-mm-thick crystal which is fully used and a 5-mm-thick crystal with an effective length of 2.5 mm. The resulting temporal resolutions of our setup are 170 fs for the 1-mm crystal and about 300 fs for the 5-mm crystal over the whole energy range. Signal dynamics over 4 orders of magnitude are attainable. The accessible energy range extends from 0.7 to 1.8 eV with an energy resolution of 35 meV limited by the spectral width of the CPM laser pulses. The spectral response of the setup is carefully calibrated with a tungsten lamp. All measurements are performed at room temperature.

III. RESULTS

A. Carrier thermalization in the coupled barrier-well system

Excitation of the heterostructures with 1.97-eV laser pulses creates hot carriers in both barriers and wells. Time-resolved luminescence spectra allow an analysis of the thermalization of this system. As an example, Fig. 2 shows time-resolved spectra of an $In_{1-x}Ga_xAs$ MQW consisting of QW's with 2.5-nm width and barriers of 30-nm width at a rather high excitation density ($n_{exc} = 6 \times 10^{12}$ cm^{-2}). This density is the two-dimensional carrier density generated within a layer consisting of one QW and one barrier. Consequently, this density would be accumulated in one QW after a transfer process of 100% efficiency. This way, we define all carrier densities in this paper. The luminescence of the $In_{1-x}Ga_xAs$ QW's is attributed to the peak at 1.05 eV

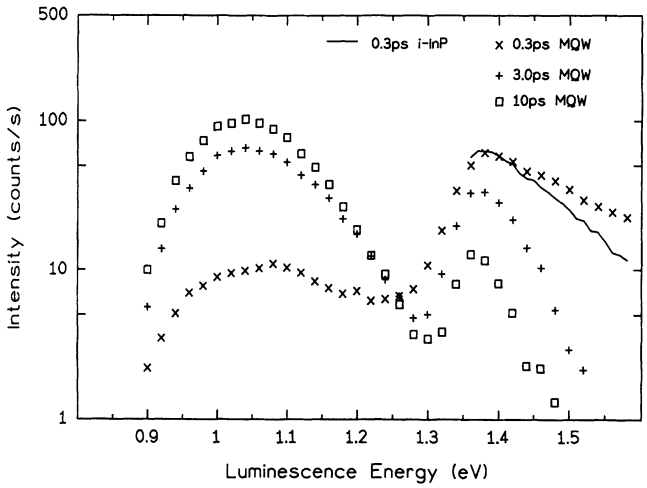

FIG. 2. Time-resolved luminescence spectra. The spectra of the 2.5/30 nm $In_{1-x}Ga_xAs$ MQW measured at different time delays after excitation are displayed by symbols. The peaks at 1.05 and 1.4 eV correspond to hot luminescence of the QW's and barriers. For comparison, a spectrum of bulk InP 300 fs after excitation is also shown (solid line).

and the luminescence of the InP barrier material to the peak at 1.4 eV. The broad line shapes reflect the hot-carrier distributions.

The luminescence spectra taken 300 fs after excitation indicate that most of the carriers are generated within the barriers. This can be expected because the barrier widths exceed the width of the QW's by more than 1 order of magnitude, while the absorption coefficients in both layers are similar. Carriers excited with 1.97-eV laser pulses in the InP barriers have excess energies of 570 meV for electrons and 50 meV for holes. In the case of the 2.5-nm $In_{1-x}Ga_xAs$ QW with an EH_1 transition of 920 meV, the excess energies are 970 and 80 meV, respectively. The offsets between bound states and InP band edges are about 100 and 320 meV for electrons and heavy holes, respectively. Therefore, heavy holes generated within the $In_{1-x}Ga_xAs$ QW's are confined, while the optically excited electrons are unbound.[36]

Maxwellian tails of both the QW and barrier luminescence are observed at time delays of 0 and 300 fs after excitation. This gives experimental proof that the thermalization of electrons and holes with high excess energies in $In_{1-x}Ga_xAs$ QW's occurs on a time scale much shorter than 300 fs. Similar ultrashort internal thermalization is observed in bulk III-V compounds by Zhou *et al.*[8,9] and, more recently, by Elsässer *et al.*[37] Due to this ultrafast thermalization, effective carrier temperatures can be evaluated at all time delays from the Maxwellian tails of the luminescence spectra. The effective carrier temperatures at 0-ps time delay of QW's and barriers (Table I) show that thermal equilibrium between QW's and barriers is established during the experimental time resolution of less than 300 fs. Already at delay $t = 0$ ps, the temperature difference between QW's and barriers is within

TABLE I. Temporal evolution of effective carrier temperatures in an 2.5/30 nm $In_{1-x}Ga_xAs/InP$ MQW and intrinsic bulk InP at an excitation density of 6×10^{12} cm^{-2} per well comparable to 2×10^{18} cm^{-3} in bulk.

Time (ps)	T_{QW} (K)	T_{bar} (K)	$T_{bulk\ InP}$ (K)
0	2400	2300	1500
0.3	2300	2200	1100
3	800	600	500
10	700	500	

the experimental error of about 100 K.

However, the temperatures observed in this MQW system are higher than in bulk InP under identical excitation conditions. Figure 2 contains for comparison an additional spectrum of bulk InP at 300 fs time delay. It is clearly visible that the barrier InP temperatures are higher than the bulk InP temperatures. Data given in Table I show that these temperature differences persists at all delay times. Possible explanations are discussed in Sec. V.

The hot QW luminescence obtained at high excitation densities of 6×10^{12} cm^{-2} exhibits a broad spectrum extending from 0.9 eV up to the InP band edge. The maximum of the QW luminescence is measured at 1.05 eV, while the EH_1 transition is observed at 0.92 eV in cw-photoluminescence experiments at low excitation densities and room temperature. This shift indicates that the bandfilling due to the very high carrier densities in the QW shifts the Fermi energies of electrons and holes and overcompensates band-gap renormalization effects.

B. Comparison of barrier decay and QW rise times

The transfer of carriers from the InP barriers to the $In_{1-x}Ga_xAs$ QW's is directly evident from the temporal evolution of the spectra. The barrier luminescence decays within picoseconds accompanied by a drastic rise of the QW luminescence, in agreement with earlier publications.[15,38,39] This indicates an ultrafast and highly efficient carrier transfer from the barriers to the QW's. The rise of the InP barrier band-edge luminescence is dominated by the carrier relaxation within the barriers and the decay by the carrier loss into the QW's. Rise and decay dynamics of a 2.5/30 nm $In_{1-x}Ga_xAs/InP$ MQW are depicted in Fig. 3. The EH_1 QW luminescence has a rise time of 4 ps from 10% to 90%. This rise time is within error identical for all structures with 30-nm barriers and well widths between 0.5 and 6 nm (see Fig. 4).

The QW luminescence rise is only partially caused by the carrier accumulation from the InP barriers. It also depends on the carrier relaxation within the QW's. We vary the excitation density over the range of 1.5×10^{11} to 6.0×10^{12} cm^{-2}. Already at excitation densities of 1.5×10^{11} cm^{-2} the quasi-Fermi-energies are close to the band edge due to the accumulation of carriers. Once the quasi-Fermi-energy has moved across the band edge, further capture fills the higher energy states. Therefore, the

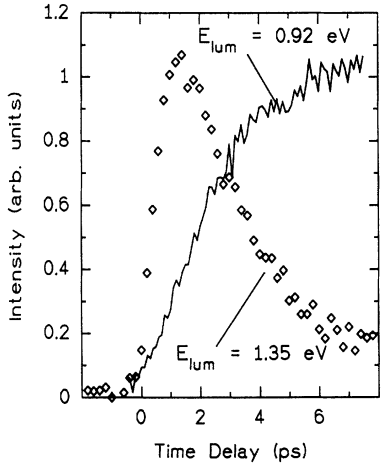

FIG. 3. Temporal evolution of the InP barrier band gap and the $In_{1-x}Ga_xAs$ EH_1 luminescence of a 2.5/30 nm MQW. Both transients are typical for all investigated structures with 30-nm barrier width.

luminescence of carriers close to the band edge does not reflect the total number of carriers in the well. Measurements of the temporal evolution up to 200 meV above the EH_1 transition show the same rise time and confirm this bandfilling effect (Fig. 5). Another effect which can delay the rise of the band-edge luminescence of the wells is the cooling of the carrier distribution leading to a slow rise.

The understanding of this cooling process might be further complicated due to the occupation of several subbands, particularly in the hole system. This complication is for observing the transfer dynamics rather than the complementary decay of the barrier luminescence. In the following discussion we therefore concentrate our investigation on the barrier luminescence decay.

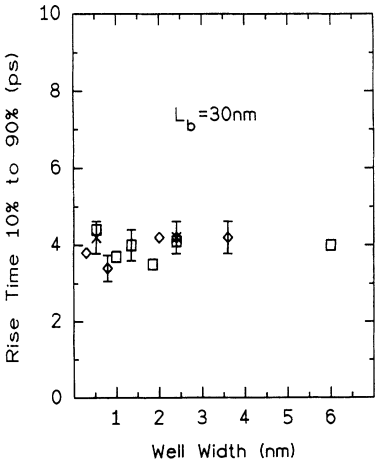

FIG. 4. Rise times (10–90%) of the EH_1 QW luminescence. The symbols depict different excitation densities of 6.0×10^{12} (squares), 7.5×10^{12} (diamonds), and 1.5×10^{12} cm^{-2} (asterisks).

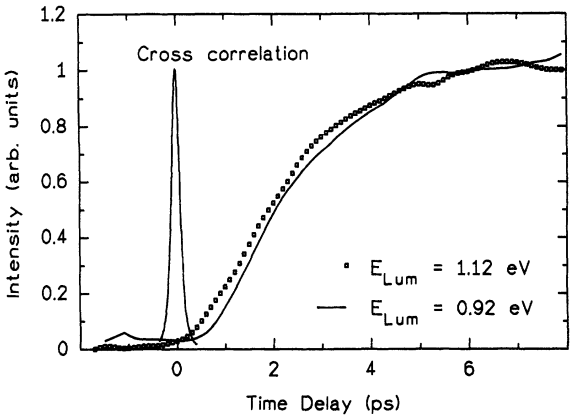

FIG. 5. Temporal evolution of the QW luminescence of a 2.5/30 nm MQW measured at different luminescence energies. The cross correlation trace demonstrates the time resolution.

C. Dependence of the carrier transfer on the well width

We study the dependence of the InP luminescence decay on well width at various excitation densities. At excitation densities of 8×10^{12} cm^{-2} and well widths of less than 1.5 nm, bandfilling of the QW states blocks the majority of the photoexcited carriers from capture into the QW's. Instead, a diffusion of the free carriers from the surface into the bulk InP substrate occurs. Decay time constants due to this vertical ambipolar plasma expansion are about 100 ps for both bulk InP and InP MQW's.[40] At excitation densities of 7.5×10^{11} cm^{-2}, most of the carriers are captured into the QW's. The decay of the InP barrier signal is more than 1 order of magnitude faster than in the case of high excitation. The decay times of structures with 30-nm barrier width are displayed in Fig. 6 as a function of well width L_z. The decay times for samples with $L_z > 2$ nm converge at 4 ps. If we reduce the excitation density to 1.5×10^{11} cm^{-2}, even the 0.5-nm well samples show this universal decay time of about 4 ps. The well width dependence of the decay times observed at the higher excitation densities obviously results from bandfilling of the QW's. *A constant decay time of 4 ps for all structures with 30-nm barrier width is obtained if the density is low enough that bandfilling is negligible.*

As mentioned above, several heavy-hole and electronic states are confined within the QW's for the well width range investigated. We do not observe the predicted oscillations in the capture time when further states are confined in the wells. A similar result was observed by Deveaud *et al.*[15]

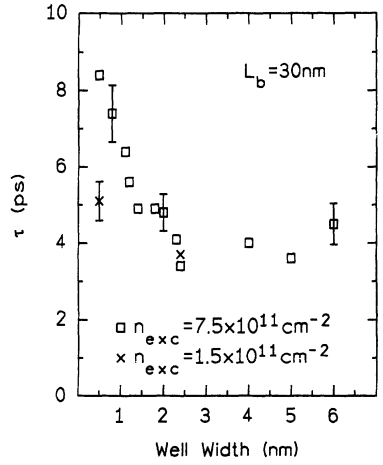

FIG. 6. Decay time constants of the barrier luminescence in dependence of well width for different excitation densities. All MQW's have an identical barrier width of 30 nm.

D. Dependence of the carrier transfer on the barrier width

To complete this study we have studied a series of samples with different barrier thicknesses. Rise times of the QW luminescence on samples with 2.5-nm well width increase with barrier width (Fig. 7). The complementary decay of InP barrier luminescence transients is slowed down to 5.2 ps as also shown in Fig. 7. A sublinear dependence on the barrier width is observed for both the QW luminescence rise and the barrier luminescence decay. Carrier diffusion across the barriers leads to transport times which scale with the square of the barrier width. An estimate of the transport time across half a 30-nm structure based on the ambipolar diffusion constant given in Ref. 19 yields 300 fs. We conclude that the transfer is not dominated by diffusive transport and that the 4-ps decay of the barrier luminescence results from carrier capture. In the next section, we perform a detailed analysis based on model calculations.

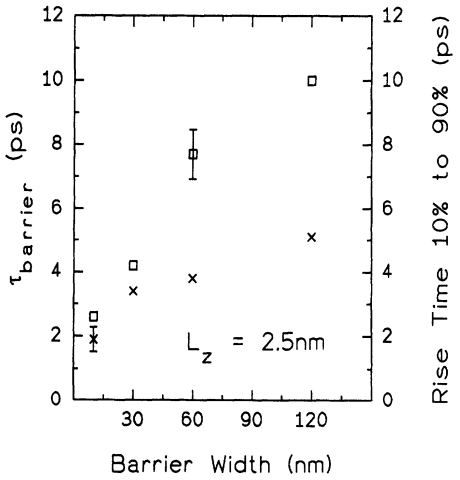

FIG. 7. Dependence of the barrier luminescence decay time (asterisks) and the QW luminescence rise (squares) on the barrier width of MQW samples with fixed well width of 2.5 nm.

IV. MODEL CALCULATION

Quantitative information about the carrier capture and about the carrier transport across the barrier material can be obtained by modeling the temporal evolution of the QW or barrier luminescence. Previous model calculations[13,14,41] are related to the temporal evolution of the QW luminescence. Quantum capture times between 100 fs and 3 ps for $GaAs/Al_xGa_{1-x}As$ structures and 4 ps for $In_{1-x}Ga_xAs/InP$ (Ref. 14) are reported. As shown previously, the decay of barrier luminescence reflects the carrier transfer to the QW's more directly than the rise of the QW luminescence. We therefore focus mainly on model calculations for the InP barrier luminescence.

In our model we assume that the capture transitions from close to the InP band edge into a confined state of the QW dominate the transfer process. This is reasonable, because capture by phonon emission or carrier-carrier scattering is much more efficient for carriers close to the band edge. Transitions far from the InP band edge into the QW's are neglected. For the carrier dynamics within the InP and the $In_{1-x}Ga_xAs$ QW's we consider only carrier relaxation processes which are relevant for the temporal evolution within the first picoseconds. Carrier recombination in $In_{1-x}Ga_xAs$ QW's (Refs. 42 and 43) and InP barriers[44] can be neglected at this time scale. The same argument is valid for vertical and lateral carrier transport[45] induced by plasma expansion, since the time constants are in the range of 100 ps to several ns. With these simplifications, we can reduce the calculation to a spatially one-dimensional model vertical to the layers and consider only the carrier transport induced by carrier capture into the QW's.

The relevant carrier dynamics included in the model are energy relaxation to the InP band edges after optical excitation, transport in direction vertical to the layers, and the capture transition into the QW's. Our simple model assumes that these processes are sequential. A more comprehensive model should treat the transfer process in an unified picture.

The excess energies of electrons and holes generated within the barriers by 1.97-eV photons are 0.57 and 0.05 eV, respectively. The energy loss is modeled by an exponential cooling process with a cooling rate of $1/\tau_{cool}$. The cooling rates of the excited carriers to the band edges are well known from previous measurements on bulk InP.[8] The cooling times are about 1 ps for electrons and depend slightly on excitation density; the time constants for holes are assumed to be about 200 fs.[46] The spatial distribution of the carrier density is constant, since the absorption length in InP (160 nm) exceeds the width of the QW period.

The carrier capture induces a density gradient of free carriers in the region of the QW's, which in turn gives rise to carrier diffusion from the barriers to the QW's. Ambipolar transport due to Coulomb attraction between electrons and holes is a realistic approximation. The ambipolar diffusion constants are derived from the mobilities published in the literature.[19]

The final part of our model is the capture process. Possible scattering processes are carrier-carrier scattering (CCS) and phonon emission. However, a compact theoretical description of scattering processes from unbound states to confined states is difficult, if a spatially inhomogeneous distribution of the carriers in the barrier is included. We therefore employ a simple model where the capture probability is proportional to the overlap of the carrier density in the barriers and the well. As a first approximation, we assume that the capture probability in real space is proportional to the square of the final wave function of the confined carrier $\Psi(z)$. The QW wave function is calculated numerically taking into account the penetration into the barriers. The rate is given by a phenomenological fit parameter, the capture time τ_{cap}.

With these approximations, we can describe the density of unbound carriers $n(z,t)$ at the InP band edge by two similar rate equations for electrons and holes,

$$\frac{\partial n(z,t)}{\partial t} = \frac{N_0}{\tau_{cool}} \exp\left(-\frac{t}{\tau_{cool}}\right) - \frac{n(z,t)}{\tau_{cap}}\Psi^2(z) + D_{amb}\frac{\partial^2 n(z,t)}{\partial z^2}. \quad (1)$$

On the right-hand side of this equation, the relaxation of the initial carrier density N_0 is described by the cooling time τ_{cool}. In the second term the carrier capture is described by the phenomenological capture time τ_{cap} and the spatial distribution proportional to the square of the wave function of a bound carrier. The carrier transport is calculated with the ambipolar diffusion constant D_{amb} using Fick's second law.

The equation is numerically solved for electrons and holes by a finite differences method in the smallest spatial element of symmetry consisting of a half barrier and a half QW. The final wave functions are approximated by Gauss functions. It should be noted that the width of the wave functions for both electrons and holes depends only slightly on the QW width. Numerical calculations have shown that this dependence can be neglected for QW's between 0.5 and 6 nm width.

Our model includes only two free parameters: the capture times of electrons and holes. They were evaluated by fits of the measured data (see Fig. 8) to be 800 ± 100 fs for electrons and 200 ± 50 fs for holes. Good agreement is achieved between all measured data of the InP luminescence and the calculation using these parameters. Figure 5 depicts the numerical results for structures with 2.5-nm QW width and barriers between 10 and 120 nm. The fit of the 2.5/30 nm structure is also representative for all structures with 30-nm barrier width and QW width between 0.5 and 6 nm, since the experimental data do not differ. One explanation for the differences between the measured and calculated curves for the sample with 120 nm width is the spatially inhomogeneous excitation density over the calculated range.

Calculations with different diffusion constants (5–50 cm^2/s) were performed to test whether the diffusive transport is restricting the carrier transfer to the QW's.

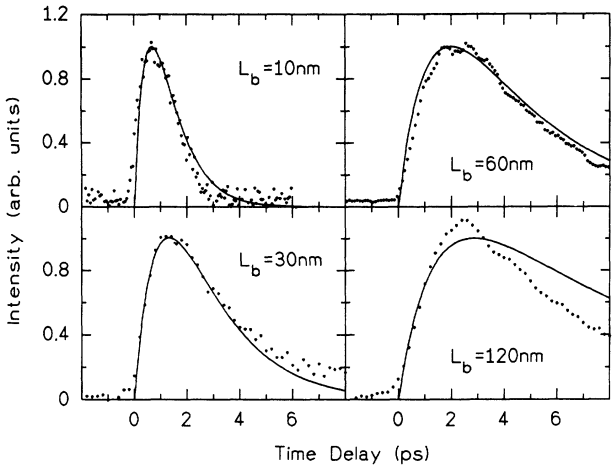

FIG. 8. Measured and calculated transients of the InP barrier luminescence of MQW's with 2.5 nm well width and various barrier widths L_b.

No significant differences were observed for the calculated dynamics at an InP barrier width of 30 nm. This result indicates that the carrier transport from the barriers to the QW's is a quasi-instantaneous process for samples with 30-nm barriers or less, in agreement with experiment and the estimated transport time. Adding drift transport to the model would therefore not lead to significant acceleration of the transport. Consequently, transfer times of several picoseconds as shown in Fig. 4 are caused only by the large ratio of the barrier width to the width of the final wave functions. The fast depletion of free carriers by capture in the small spatial region of the QW's is instantaneously compensated by transport from the barriers. Since the width of the barriers exceeds that of the QW's, this depletion reduces the number of carriers within the barriers slowly and picosecond decay times are observed.

The differences in the phenomenological capture times for electrons and holes do not lead to a significant difference in the overall trapping rate: The smaller capture time of holes is compensated by the larger spatial extent of the electron wave function. Therefore electrons and holes are captured with similar overall rates into the QW's.

V. DISCUSSION

In this section, we summarize our results and compare them with the literature. We found that the carriers thermalize to Fermi-Dirac distributions within time resolution (300 fs). Nearly identical carrier temperatures in the $In_{1-x}Ga_xAs$ QW's and the InP barriers are established on the same time scale. Both observations depict the strong interactions between carriers in both materials and the resulting ultrafast energy exchange. However, much higher carrier temperatures are observed in the barrier InP compared to bulk InP. This can result from different processes: First, the carrier distribution within the InP barriers can be heated by the interaction with hot carriers in the QW's. Energy transfer processes by CCS between carriers of QW's and barriers and by LO phonon emission within the QW's and subsequent absorption within the barriers are possible.[47–52] Second, a heating of the carrier distribution may also result from a preferential capture of carriers which are energetically close to the InP band edges. This can be expected because carrier capture processes by phonon emission as well as by carrier-carrier interactions are more effective near the band edges. Thus the carrier distribution in the InP barriers is heated by the transfer of carriers with low kinetic energy into the QW's. This heating process is similar to recombination heating in bulk materials. A third effect is the difference in carrier statistics between barriers and wells: In the barriers the average energy of the carriers is $\frac{3}{2}kT$, in the QW's kT. Carrier transfer from barriers to wells will therefore lead to an increased carrier temperature.

A carrier transfer in real space is only possible if the Fermi energies or the temperatures between both regions differ. The nearly identical carrier temperatures from the moment of excitation in QW's and barriers show that the transfer is only controlled by the difference of the quasi-Fermi-energies. Accordingly, the carrier transfer must have started when thermal equilibrium is reached after 300 fs. The accumulation of carriers within the QW's stops, when the Fermi energies of QW's and barriers become equal.

Before comparing our data with data published in the literature, we have to discuss the dependence of the capture and transport process on the lattice temperature. The transfer process is completed within several picoseconds after excitation. Within this time regime, a thermal equilibrium between carriers and lattice cannot be established, whether the sample is cooled or held at room temperature. This indicates that the lattice temperatures should be rather unimportant for the trapping rates. The temporal evolutions of both QW and barrier luminescence obtained by Deveaud *et al.*[15] at 70 and 150 K indeed agree with ours measured at room temperature. Reihlen *et al.*[19] also did not observe a dependence of the capture efficiency on the sample temperature in cw-photoluminescence experiments.

The investigation of the temporal evolutions of both barrier and QW luminescence do not show a dependence of the transfer rate on well width. This disagrees with theoretical studies which predict extrema of the capture rate, when a further electronic state is confined within the QW's enlarging the well width. We have performed detailed calculations of the confined states using the transfer matrix method as published by Juillaguet *et al.*[53] The band nonparabolicity of the conduction band has been taken into account in the framework of the Kane model.[54] The detailed interface structure of the samples has been included.[55] The calculations for the investigated well width show that several heavy-hole states and up to two electron states are confined within the QW's. For a QW width of 6 nm the second electron state is confined. We measure the same transfer rates at all well widths,

regardless of the location of confined levels for electrons or holes in the QW's.

Model calculations of the carrier dynamics within the QW's are much more involved than calculations of bulk material. Several calculations modeling the experimental data of the QW luminescence have yielded the broad spectrum of capture times published for $In_{1-x}Ga_xAs/InP$ and $GaAs/Al_xGa_{1-x}As$.[10,13,14,41] Calculations of the barrier luminescence as performed in this paper circumvent the problem of intra-QW relaxation. However, we should point out that our model is still based on some crude approximations. In particular, the assumption of a capture rate proportional to the spatial density of the final wave function has to be improved. Nevertheless, quantitative fits of all barrier luminescence data as well as qualitative fits of the QW luminescence data are possible with the same capture times of 800 fs for electrons and 200 fs for holes.

It is striking that the evaluated capture times are generally smaller than those predicted by the theoretical works based on phonon emission.[22–24] One reason for the discrepancy could be the additional contribution of other scattering processes, in particular CCS. Such many-body effects have been discussed in detail in Ref. 56. The measurements of Ref. 56 were done at very high densities (10^{19} cm^{-3}). A study of the dependence of the capture time on density with our method is limited by the detection sensitivity of the upconversion setup. In the density range studied (1.5×10^{11} to 6.0×10^{12} cm^{-2}), no significant dependence was observed.

The dependence of the QW luminescence rise time on the barrier width is obvious from the results of our model calculations: The fast capture in the region of the QW's depletes the barriers. In the case of large barriers, this depletion needs more time than for smaller barriers. In contrast to Ref. 15, we do not find a significant retardation by diffusion for barrier widths up to 30 nm. One would expect that for 120-nm barriers, carrier diffusion (4.5 ps for the half barrier width of 60 nm) has to be taken into account. However, we find a sublinear dependence of the transfer time on the barrier width (Fig. 7), indicating that diffusion is still unimportant. The extremely large QW luminescence rise times of hundreds of picoseconds as published in Refs. 10, 14, and 57 can be explained by diffusion across cap layers with a thickness of up to several micrometers or by the energy relaxation of the excitons to $\mathbf{k} = 0$.[58]

If the barrier width does not exceed 30 nm, the diffusive term of the rate equation [Eq. (1)] can be neglected. Consequently, the carrier loss of the barriers can be directly described by the spatial integral of the local capture rate given by $\Psi^2(z)/\tau_{cap}$. We then obtain for the transfer rate

$$\frac{1}{\tau_{transfer}} = \frac{2}{L_b + L_z} \int_0^{(L_b+L_z)/2} \frac{\Psi^2(z)}{\tau_{cap}}\, dz. \qquad (2)$$

Electron and hole transfer times of about 5 ps are deduced. Ambipolar transfer can be expected due to the strong Coulomb forces between electrons and holes. Similar transfer times were obtained by a preliminary model as published in our previous work.[16] Equation (2) is a simple formalism to calculate the carrier transfer time for structures with barrier widths up to 30 nm and well widths between 0.5 and 6 nm. In general, ultrafast devices can be obtained independent of well width if the barrier width does not exceed 30 nm. As depicted in Fig. 4, the QW luminescence rise of 2.5 ps allows modulation frequencies on the order of 300 GHz.

VI. CONCLUSION

The carrier transport and capture properties in $In_{1-x}Ga_xAs/InP$ MQW's are investigated by upconversion luminescence experiments with femtosecond time resolution. Carrier transport through the InP barrier layers and carrier capture into the QW's are separated. The dynamics of the QW luminescence is influenced by carrier relaxation and bandfilling processes, which might obscure the dynamics due to carrier capture. The charge transfer is more directly observed by the InP barrier luminescence decay. A detailed investigation of the barrier luminescence decay yields decay times of 4 ps for all well widths investigated at a fixed barrier width of 30 nm. No oscillations or a dependence of the transfer time on well width as predicted by theoretical studies are observed.

Measurements on MQW samples with barrier widths between 10 and 120 nm and a comparison to model calculations yield detailed information about carrier transport and capture processes. The capture times obtained are about 800 fs for electrons and 200 fs for holes. The transport of carriers through the InP barrier material occurs quasi-instantaneously by ambipolar diffusion in samples with moderate barrier widths. Therefore, graded gap structures of only several nm thickness are not expected to accelerate the transport to the QW's. Our measurements performed at lattice temperatures and excitation densities similar to those to be used in future devices demonstrate the ultrafast carrier dynamics within MQW structures. The carrier transfer to the QWs' is completed within 3 ps in structures with barrier widths of 10 nm or less. Consequently, the charge transfer is not expected to limit the modulation frequency of devices below 300 GHz.

ACKNOWLEDGMENTS

We like to thank D. Grützmacher and M. Stollenwerk for sample preparation, B. Gallmann for cw characterization, H. J. Bakker for helpful discussions, and X. Q. Zhou for technical help and discussions. The financial support by the Deutsche Forschungsgemeinschaft (Contract No. Ku 540/6-3) and the Alfried-Krupp-Stiftung is gratefully acknowledged.

[1]K. Kash and J. Shah, Appl. Phys. Lett. **45**, 401 (1984).
[2]D. J. Westland, R. F. Ryan, M. D. Scott, J. I. Davis, and J. R. Riffat, Solid State Electron. **31**, 431 (1988).
[3]W. Kütt, K. Seibert, and H. Kurz, in *High Density Femtosecond Excitation of Hot Carrier Distributions in InP and InGaAs*, edited by T. Yajima, K. Yoshihara, C. B. Harris, and S. Shinoya, Springer Series in Chemical Physics Vol. 48 (Springer-Verlag, Berlin, 1988).
[4]H. Kurz, W. Kütt, K. Seibert, and M. Strahnen, Solid State Electron. **31**, 447 (1988).
[5]H. Lobentanzer, W. Stolz, J. Nagle, and K. Ploog, Phys. Rev. B **39**, 5234 (1989).
[6]J. Shah, B. Deveaud, T. C. Damen, W. T. Tang, A. C. Gossard, and P. Lugli, Phys. Rev. Lett. **59**, 2222 (1987).
[7]J. Shah, Superlatt. Microstruct. **6**, 293 (1989).
[8]X. Q. Zhou, U. Lemmer, K. Seibert, G. C. Cho, W. Kütt, K. Wolter, and H. Kurz, Proc. SPIE **1268**, 166 (1990).
[9]X. Q. Zhou, U. Lemmer, K. Seibert, G. C. Cho, W. Kütt, K. Wolter, and H. Kurz, in *20th International Conference on the Physics of Semiconductors, Thessaloniki, Greece*, edited by E. M. Anastassakis and J. D. Joannopoulos (World Scientific, Singapore, 1990), Vol. 3, p. 2552.
[10]E. O. Göbel, H. Jung, J. Kuhl, and K. Ploog, Phys. Rev. Lett. **51**, 1588 (1983).
[11]J. Feldmann, G. Peter, E. O. Göbel, K. Leo, H.-J. Polland, K. Ploog, K. Fujiwara, and T. Nakayama, Appl. Phys. Lett. **51**, 226 (1987).
[12]H.-J. Polland, K. Leo, K. Rother, K. Ploog, J. Feldmann, G. Peter, E. O. Göbel, K. Fujiwara, T. Nakayama, and Y. Otha, Phys. Rev. B **38**, 7635 (1988).
[13]P. W. M. Blom, R. F. Mols, J. E. M. Haverkort, M. R. Leys, and J. H. Wolter, Superlatt. Microstruct. **7**, 319 (1990).
[14]D. J. Westland, D. Mihailovic, J. F. Ryan, and M. D. Scott, Appl. Phys. Lett. **51**, 590 (1987).
[15]B. Deveaud, J. Shah, T. C. Damen, and W. T. Tsang, Appl. Phys. Lett. **52**, 1886 (1988).
[16]R. Kersting, X. Q. Zhou, K. Wolter, D. Grützmacher, and H. Kurz, Superlatt. Microstruct. **7**, 345 (1990).
[17]J. Christen, D. Bimberg, A. Steckenborn, and G. Weimann, Appl. Phys. Lett. **44**, 84 (1984).
[18]D. Bimberg, J. Christen, A. Steckenborn, G. Weimann, and W. Schlapp, J. Lumin. **30**, 562 (1985).
[19]E. H. Reihlen, A. Persson, T. Y. Wang, K. L. Fry, and G. B. Stringfellow, J. Appl. Phys. **66**, 5554 (1989).
[20]N. Ogasawara, A. Fujiwara, N. Ohgushi, S. Fukatsu, Y. Shiraki, Y. Katayama, and R. Ito, Phys. Rev. B **42**, 9562 (1990).
[21]A. Fujiwara, S. Fukatsu, Y. Shiraki, and R. Ito (unpublished).
[22]J. A. Brum and G. Bastard, Phys. Rev. B **33**, 1420 (1986).
[23]M. Babiker and B. K. Ridley, Superlatt. Microstruct. **2**, 287 (1986).
[24]M. Babiker, M. P. Chamberlain, A. Ghosal, and B. K. Ridley, Surf. Sci. **196**, 422 (1988).
[25]P. W. M. Blom, J. E. M. Haverkort, and J. H. Wolter, Appl. Phys. Lett. **58**, 2767 (1991).
[26]D. Grützmacher, K. Wolter, C. W. T. Bulle Lieuwma, H. Jürgensen, and P. Balk, Appl. Phys. Lett. **52**, 872 (1988).
[27]D. Grützmacher, J. Hergeth, F. Reinhardt, K. Wolter, and P. Balk, J. Electron. Mater. **19**, 471 (1990).
[28]M. Zachau and D. Grützmacher, Appl. Phys. Lett. **56**, 632 (1990).
[29]J. P. Laurenti, J. Camassel, B. Reynes, D. Grützmacher, K. Wolter, and H. Kurz, Semicond. Sci. Technol. **5**, 222 (1990).
[30]A careful comparison of the luminescence results with model calculations indicates that the growth interruption sequence leads to additional layers at the $In_{1-x}Ga_xAs$ interfaces. For the samples used in this work, additional 2 ML $InAs_{0.65}P_{0.35}$ and 2 ML InGaAs:P with unknown composition were found [J. Camassel, J. P. Laurenti, S. Juillaguet, F. Reinhardt, K. Wolter, H. Kurz, and D. Grützmacher, J. Cryst. Growth **107**, 543 (1991); R. Schwedler, B. Gallmann, K. Wolter, D. Grützmacher, M. Stollenwerk, and H. Kurz, in *Proceedings of the International Conference on Advanced Materials, ICAM 91, Strassburg, 1991,* edited by K. J. Bachman, H.-L. Hwang, and C. Schwab (Elsevier, New York, 1992)]. The effect of these intermediate layers can be included as an apparent increase of the QW width by about 1.2 nm. In the following text, however, we denote the QW width by the width of the $In_{1-x}Ga_xAs$ layers only.
[31]D. Hulin, A. Mingus, A. Antonetti, I. Ledoux, J. Badan, J. L. Oudar, and J. Zyss, Appl. Phys. Lett. **49**, 761 (1986).
[32]J. Shah, T. C. Damen, B. Deveaud, and D. Block, Appl. Phys. Lett. **50**, 1307 (1987).
[33]J. Shah, IEEE J. Quantum Electron. **24**, 276 (1988).
[34]R. L. Fork, B. I. Greene, and C. V. Shank, Appl. Phys. Lett. **38**, 671 (1981).
[35]J. A. Valdmanis and R. L. Fork, IEEE J. Quantum Electron. **22**, 112 (1986).
[36]We note that a detailed inclusion of the full valence-band structure might lead to a different distribution of the excess energy.
[37]T. Elsässer, J. Shah, L. Rota, and P. Lugli, Phys. Rev. Lett. **66**, 1757 (1991).
[38]D. Y. Oberli, J. Shah, J. L. Jewell, and T. C. Damen, Appl. Phys. Lett. **54**, 1028 (1989).
[39]B. Deveaud, F. Clerot, A. Regreny, K. Fujiwara, K. Mitsunaga, and J. Otha, Appl. Phys. Lett. **55**, 2646 (1989).
[40]K. Wolter, R. Schwedler, F. Reinhardt, R. Kersting, X. Q. Zhou, D. Grützmacher, and H. Kurz, in *Proceedings ESSDERC 90, 20th European Solid State Device Research Conference, Nottingham*, edited by W. Eccleston and P. J. Rosser (Hilger, Bristol, 1990), p. 405.
[41]A. Weller, P. Thomas, J. Feldmann, G. Peter, and E. O. Göbel, Appl. Phys. A **48**, 509 (1989).
[42]U. Cebulla, G. Bacher, A. Forchel, G. Mayer, and W. T. Tsang, Phys. Rev. B **39**, 6257 (1989).
[43]U. Cebulla, G. Bacher, G. Mayer, A. Forchel, W. T. Tsang, and M. Razeghi, Superlatt. Microstruct. **5**, 227 (1989).
[44]J. Bokor, R. H. Storz, J. Stark, R. R. Freeman, and P. H. Buchsbaum, Phys. Rev. B **32**, 3669 (1985).
[45]H. Hillmer, S. Hansmann, A. Forchel, M. Morohashi, E. Lopez, H. P. Meier, and K. Ploog, Appl. Phys. Lett. **53**, 1937 (1988).
[46]X. Q. Zhou, K. Leo, and H. Kurz, Phys. Rev. B **45**, 3886 (1992).
[47]J. Shah and R. F. Leheny, in *Semiconductors Probed by Ultrafast Laser Spectroscopy*, edited by R. R. Alfano (Academic, New York, 1984).
[48]M. Asche and O. G. Sarbei, Phys. Status Solidi B **126**, 607 (1984).
[49]M. Asche and O. G. Sarbei, Phys. Status Solidi B **141**, 487 (1987).
[50]R. A. Höpfel, J. Shah, and A. C. Gossard, Phys. Rev. Lett.

56, 765 (1986).
[51]M. A. Osman and D. K. Ferry, Phys. Rev. B **36**, 6018 (1987).
[52]M. A. Osman, M. Cahay, and H. L. Grubin, Solid State Electron. **32**, 1911 (1989).
[53]S. Juillaguet, J. P. Laurenti, R. Schwedler, K. Wolter, J. Camassel, and H. Kurz, in *Proceedings ICAM 91, Strassburg, 1991* (Ref. 30), p. 155.
[54]E. O. Kane, J. Phys. Chem. Solids **1**, 249 (1957).
[55]J. Camassel, J. P. Laurenti, S. Juillaguet, F. Reinhardt, K. Wolter, H. Kurz, and D. Grützmacher, J. Cryst. Growth **107**, 543 (1991).
[56]S. Weiss, J. M. Wiesenfeld, D. S. Chemla, G. Raybon, G. Sucha, M. Wegener, G. Eisenstein, C. A. Burrus, A. G. Dentai, U. Koren, B. I. Miller, H. Temkin, R. A. Logan, and T. Tanbun-Ek, Appl. Phys. Lett. **60**, 9 (1992).
[57]H.-J. Polland, K. Leo, K. Ploog, J. Feldmann, G. Peter, E. O. Göbel, K. Fujiwara, and T. Nakayama, Solid State Electron. **31**, 341 (1988).
[58]T. C. Damen, J. Shah, D. Y. Oberli, D. S. Chemla, J. E. Cunningham, and J. M. Kuto, Phys. Rev. B **42**, 7434 (1990).

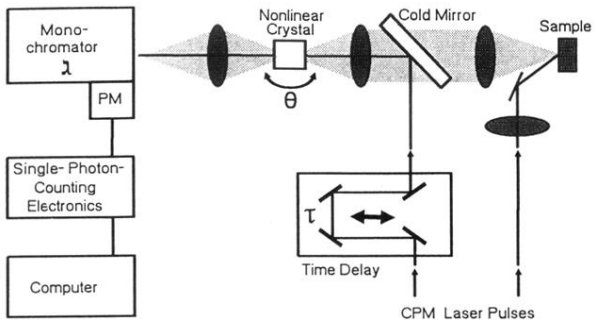

FIG. 1. Luminescence upconversion setup.